Chinese Chemical Letters 36 (2025) 110321

Contents lists available at ScienceDirect

Chinese Chemical Letters

journal homepage: www.elsevier.com/locate/cclet

Recent progress of tailoring valuable graphene quantum dots from biomass

Tong Zhao, Ke Wang, Feiyu Liu, Shiyu Zhang, Shih-Hsin Ho*

State Key Laboratory of Urban Water Resource and Environment, School of Environment, Harbin Institute of Technology, Harbin 150090, China

ARTICLE INFO

Article history:
Received 29 March 2024
Revised 3 July 2024
Accepted 6 August 2024
Available online 8 August 2024

Keywords:
Carbon nanomaterials
Graphene quantum dots
Biomass resources
Green synthesis
Properties
Applications

ABSTRACT

Graphene quantum dots (GQDs) are a class of promising carbon-based nanomaterials that have attracted considerable interest from researchers due to their excellent physical, chemical, and biological properties. However, the high cost, toxicity, and laborious preparation process of GQDs also limit their widespread use. To address this issue, the actual research directions consist in replacing traditional non-renewable feedstocks *via* screening cheap, easily available, and renewable biomass materials based on the concept of resource conservation and environmental friendliness. Herein, the state-of-the-art technologies in the green preparation of GQDs using biomass as carbon source are reported. Initially, the green synthesis strategies as well as the structural, optical, and biosafety properties of GQDs are discussed in detail. Subsequently, the most representative applications of GQDs in energy and environmental remediation fields are summarized. Finally, the current challenges and future potential of the GQDs are presented.

1. Introduction

As one of the most plentiful and essential biological elements, carbon and its allotropes have been widely scrutinized by the academic community [1-3]. Since the discovery of fullerenes to the era of carbon nanotubes (CNTs), graphene and other relevant two-dimensional (2D) carbon nanomaterials, a considerable breakthrough has been achieved in the advancement of materials science and nanotechnology [4]. Among carbon-based nanomaterials, a carbon heteromorphic material, graphene, is a burgeoning superstar in the field of materials science, being considered a revolutionary material of the future [5]. This innovative material is made of carbon atoms *via* sp^2 hybridization, which are densely packed into a single-atom layer-thick 2D hexagonal honeycomb lattice structure. Such highly ordered, closely-arranged layer of single-molecule carbon atoms endows graphene with excellent mechanical, thermal, electrical and optical properties, which have broad application prospects since its discovery in 2004 [6]. In spite of extensive research on graphene, several shortcomings have been encountered, including zero band gap, limited spectral absorption, and poor dispersibility in organic solvents [7]. Since the deeper investigations of the graphene family, the discovery of graphene quantum dots (GQDs) in 2008 has promoted a huge advancement in addressing these challenges (Fig. 1a) [8–17].

GQDs are zero-dimensional (0D) graphene nanofragments whose lateral dimensions are typically less than 10 nm. In addition to inheriting the outstanding characteristics of graphene materials, including large specific surface area, enhanced carrier mobility and high stability, GQDs also exhibit excellent optoelectronic properties, which makes them ideal materials for optoelectronic devices [18,19]. Compared with other quantum dots that are able to fluoresce in the visible light range, GQDs possess tunable fluorescence properties, surface functionalization feasibility, and high photoluminescence performance. What's more, they are also more stable in aqueous solutions [20]. Besides, compared with other traditional semiconductors, GQDs exhibit biocompatibility and no obvious toxicity [21,22]. Consequently, GQDs are highly promising in the detection and removal of contaminants from the environment (Figs. 1b and c) [23–27]. Many strategies have been devised for synthesizing GQDs, including top-down approaches starting from graphene or CNTs and bottom-up approaches using small molecules as precursors [28]. Nevertheless, most of these strategies tend to use expensive non-renewable precursors or require toxic and hazardous chemical reagents that impose risks on human safety and environment, which limits their sustainable development and widespread application [29]. Therefore, green synthesis methods utilizing environmentally friendly solvents and renewable raw materials to reduce energy consumption and chemical waste formation are becoming increasingly essential.

* Corresponding author.
E-mail address: stephen6949@hit.edu.cn (S.-H. Ho).

https://doi.org/10.1016/j.cclet.2024.110321
1001-8417/

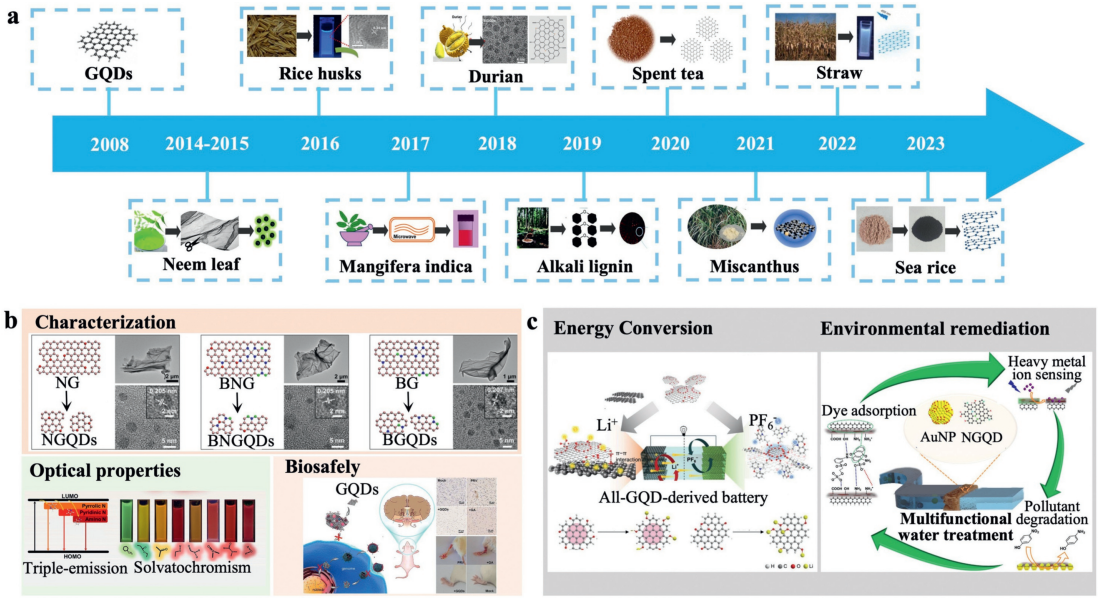

Fig. 1. (a) Development of biomass-derived GQDs. Copied with permission [9]. Copyright 2014, the Royal Society of Chemistry. Copied with permission [10]. Copyright 2016, American Chemical Society. Copied with permission [11]. Copyright 2017, American Chemical Society. Copied with permission [12]. Copyright 2018, American Chemical Society. Copied with permission [13]. Copyright 2019, the Royal Society of Chemistry. Copied with permission [14]. Copyright, Springer Nature. Copied with permission [15]. Copyright 2021, Elsevier. Copied with permission [16]. Copyright 2022, Elsevier. Copied with permission [17]. Copyright 2023, Elsevier. (b) Properties of current GQDs. Copied with permission [23]. Copyright 2022, American Chemical Society. Copied with permission [24]. Copyright 2022, Elsevier. Copied with permission [25]. Copyright 2024, the Royal Society of Chemistry. (c) Applications of current GQDs. Copied with permission [26]. Copyright 2023, John Wiley and Sons. Copied with permission [27]. Copyright 2023, Elsevier.

The abundant and easily accessible biomass is considered a safe, sustainable, and eco-friendly natural source of organic carbon. Numerous attempts have been made to use biomass as a carbon source to produce GQDs in an environmentally friendly way since 2014 [9]. In contrast to conventional GQDs, biomass derived-GQDs allow for waste management and value addition while reducing dependence on fossil fuels. Moreover, biomass-derived precursors usually contain heteroatoms such as oxygen and nitrogen, which can enhance the photoluminescent properties of synthesized GQDs.

Biomass-derived GQDs are widely applied in optoelectronic devices, sensors, photocatalysis, and other areas. However, obtaining GQDs with exceptional properties and high yields from complex biomass is still a challenging task. Green synthesis methods, performance modulation and application expansion of biomass-derived GQDs need to be further investigated. In this review, the green synthesis strategies for the preparation of GQDs from biomass and the structural, optical, and biosafety features of biomass-derived GQDs in recent years are systematically analyzed. Simultaneously, the potential applications of biomass-derived GQDs are demonstrated in energy and environmental remediation fields. Ultimately, the challenges encountered upon the use of biomass-derived GQDs are discussed and future research directions are proposed, setting the groundwork for the advancement of high-quality carbon materials.

2. Green synthesis of GQDs from biomass

A variety of synthesis strategies of GQDs have been developed to date (Fig. 2). In accordance with the reaction mechanism, the synthesis of GQDs mainly consists in top-down and bottom-up strategies. Top-down synthesis methods use graphitized carbon materials, which are exfoliated or cut into GQDs *via* oxidation. Although the relevant processes are favorable for large-scale production, they usually require strong oxidants that are harmful to the environment and do not allow controlling the morphology of GQDs precisely [30]. In comparison, bottom-up synthesis methods mostly

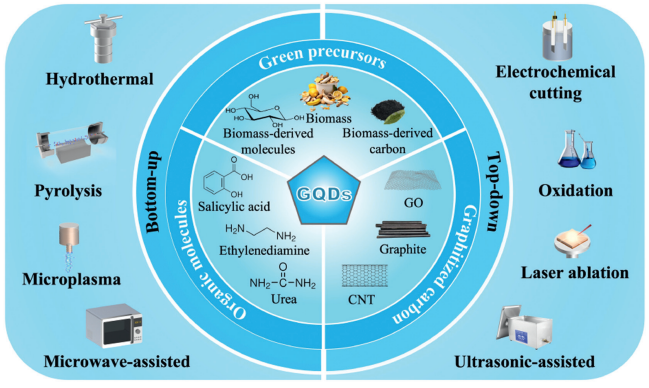

Fig. 2. Illustration of methods for GQDs synthesis.

use small molecules to synthesize GQDs [31]. Meanwhile, in spite of advantages such as low cost and environmental protection, specific organic materials are often needed. Therefore, focusing on renewable feedstocks is expected to produce GQDs from natural resources through a bottom-up green route.

Inexpensive, straightforward, and eco-friendly green synthesis techniques have aroused a great deal of interest as an emerging alternative to traditional technologies [32,33]. Thanks to the diversity of biomass, various attempts have been made to produce GQDs through green synthesis approaches. In particular, the extraction of molecules from biomass upon the synthesis of GQDs is realized along the bottom-up strategy. In addition, biomass can be thermally treated to produce turbostratic carbon. Continuous thermal treatment of this disordered carbon is anticipated to result in the large-scale production of GQDs [34]. To account for the characteristics of biomass, up-down joint methods have been developed, whereby carbon is first generated through the bottom-up route and is then utilized to synthesize GQDs *via* the top-down route. Table 1 [11,12,15-17,35-45] displays the precursors, methods,

Table 1
Precursors, methods, properties, and applications of GQDs from biomass.

Biomass	Approach	Treatment parameter	Yield	Size (nm)	Quantum yield (QY)	Application	Ref.
Paddy straw	Hydrothermal	160 °C, 6 h	–	5–15	–	–	[35]
Sugarcane bagasse	Hydrothermal	140–180 °C, 0–4 h	–	2.26 average	–	–	[36]
Miscanthus	Hydrothermal	120 °C, 12 h	19.8 wt%	4.05 ± 0.61	54%	Detection of Fe^{3+}	[15]
Cotton	Hydrothermal	180 °C, 8 h	57.7%	1.0–5.0	19.4%	Bioimaging	[37]
Passiflora edulia Sims	Hydrothermal	180 °C, 4 h	–	3.8 average	29%	Sensing, fluorescence ink and multicolor cell imaging	[38]
Corn straw	Hydrothermal	170 °C, 12 h		1.5–4.0	15.65%	Detection of PO_4^{3-}	[16]
Starch	Hydrothermal	190 °C, 2 h	–	5 average	–	Accelerate the healing of wounds	[39]
Brewer's spent grains	Hydrothermal	150 °C, 14 h	–	–	0.29%	Photodegradation of methyl orange	[40]
Date palm tree leaves	Hydrothermal	200 °C, 12 h	52%	3.5–8	–	–	[41]
Durian	Hydrothermal	150 °C, 12 h, with platinum catalyst	6.8 wt%	2–6	79%	–	[12]
Spent black tea bags	Hydrothermal	200 °C, 12 h with ethanol	–	0.5–4	21%	Optical sensing probe	[42]
Lemon juice	Ultrasound-assisted hydrothermal	220 °C, 72 h	–	20 average	–	–	[43]
Melamine sponge and arjuna bark	Microwave	700 W, 10 min	72.5 wt%	2–3	8.5%	Cell imaging and H_2O_2 sensing	[11]
Mangifera indica	Microwave	900 W, 5 min	–	2–8	–	Near-infrared bioimaging and intracellular nanothermometry	[17]
Sea rice	Mild oxidation	H_2O_2 (30%)	–	1.20 ± 0.40 average	–	Detection of 4-nitrophenol	[44]
Chitosan	Microplasma	9.6 mA discharge current	50%	4.36 ± 0.92 average	–	Environmental-responsive nanosensors and nanothermometers	[45]

properties, and applications of biomass-derived GQDs prepared by green synthesis strategies.

2.1. Hydrothermal/Solvothermal method

The hydrothermal/solvothermal method is the most popular way for green synthesis of GQDs due to its convenient operation and mild reaction conditions. This method enables the synthesis of GQDs from natural precursors, such as citric acid (CA), glucose and biowaste, at relatively low temperature and saturation pressure [46,47]. Feedstock and reaction conditions are the key parameters during the synthesis of GQDs. The hydrothermal conversion is usually carried out *via* dehydration, polymerization, and carbonization reactions [48]. Biomass containing cellulose, hemicellulose, lignin and proteins is initially hydrolyzed to monosaccharide units, which are then subjected to decomposition and polymerization-polycondensation reactions [49]. For complex biomass, incomplete hydrolysis of the feedstock results in the inhomogeneous products, and multiple materials can be obtained. In addition, biomass usually contains a large amount of sulfur, nitrogen, and other elements. The doping element reactions can occur simultaneously during hydrothermal reactions, leading to the emergence of abundant functional groups on the surface of GQDs. GQDs can also be functionalized by adding functional reagents during the synthesis [50].

Some derivatives obtained from biomass can be used as simple precursors to synthesize GQDs in hydrothermal reactions. In particular, CA extracted from citrus fruits can be used as a small molecule for the synthesis of GQDs [51,52]. Zhu *et al.* [53] used CA as a carbon source to prepare N-GQDs with high quality and quantum yield (QY) up to 54%. CA can self-assemble into lamellar structures and dehydrate to form graphene skeletons, and the degree of carbonization can be modulated by varying the hydrothermal reaction time. Lignin as part of trees and herbaceous plants is a biomass material that naturally contains aromatic compounds [54-56]. During the hydrothermal process, lignin is cleaved into aromatic monomers, which are then transformed into polycyclic aromatic hydrocarbons, and the sp^3 carbon atom is converted to the sp^2 one (Fig. 3a). In addition, the increase in the alkalinity of the reaction environment favors lignin cleavage and aromatic molecule aggregation [50]. Intriguingly, sulfur-containing industrial lignin structures can also be used for the synthesis of S-GQDs, which will further broaden the application scope of GQDs [57]. Furthermore, Chen *et al.* [37,58] prepared GQDs from natural polymers, such as starch or cellulose, which involved the hydrolysis of feedstocks and the ring-closure condensation of glucose. The only products that are released in this method are GQDs, water and carbide precipitation, without any pollutants generated (Fig. 3b).

GQDs can be synthesized from fruit wastes. For example, *Passiflora edulia Sims* is rich in sugars such as glucose and fructose. When exposed to hydrothermal treatment, it is able to produce multicolor luminescent N-GQDs with desirable ionic stability, hydrophilicity, and resistance to photocleavage [38]. Similarly, the small-molecule sugars present in durian can be used as a carbon source to form the sp^2 carbon framework within GQDs [12]. It is noteworthy that thiols as part of durian ensure lattice doping of elemental sulfur during the hydrothermal process, and their concentration can be modulated by varying the reaction time and temperature so as to remove heteroatoms. Sulfur doping not only provides favorable photochemical/chemical stability, but also ultra-high QY (79%).

Agricultural and forestry wastes are mostly composed of cellulose, hemicellulose and lignin, which are commonly used precursors for GQDs synthesis. Bagasse, mainly composed of lignocellulose with low ash content, has great potential in the preparation of carbon materials. GQDs, fermentable sugars and layered porous carbon can be generated simultaneously in hydrothermal processes depending on the complex composition of bagasse. The rich benzene ring structure in polysaccharides and lignin provides the basis for the production of GQDs. Bagasse-derived GQDs obtained *via* hydrothermal method have a small average diameter (2.26 nm) and a clear graphite structure. The abundant oxygen groups at the edge of the carbon layer make GQDs optically stable with excellent water solubility [36]. Rice husks contain organic matter such as lignocellulose, pentosan and high-quality concentrations of silicas. Analogous to bagasse, the organics matter in rice husks can

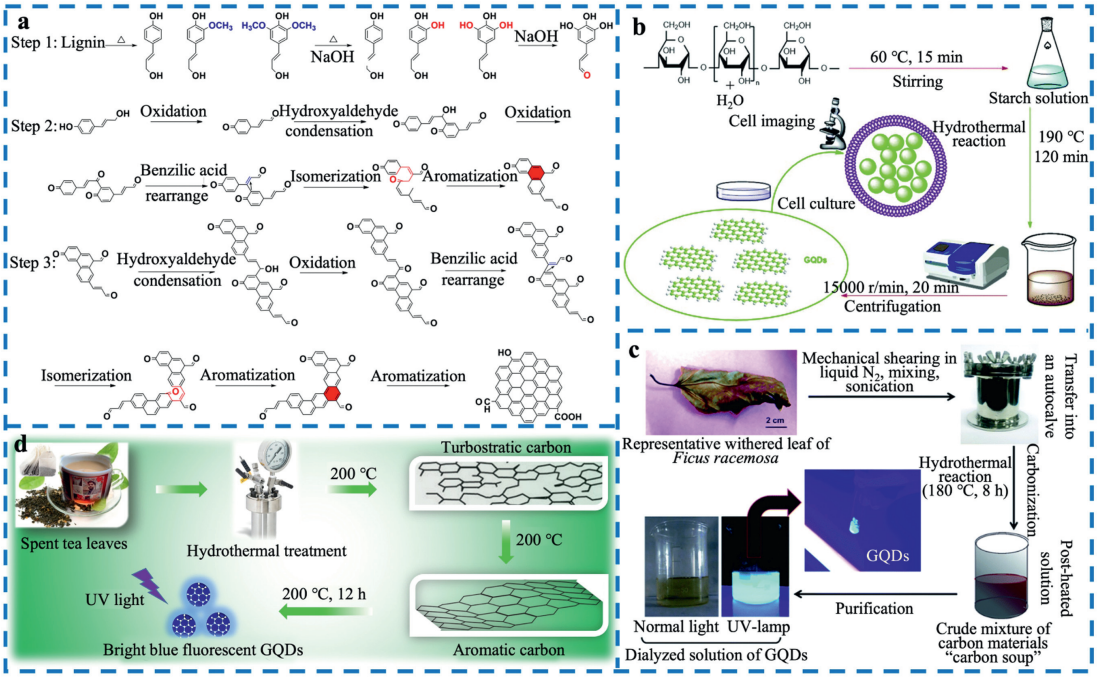

Fig. 3. Schematic demonstration of the hydrothermal/solvothermal process of GQDs from (a) lignin. Copied with permission [50]. Copyright 2023, the Royal Society of Chemistry. (b) starch. Copied with permission [58]. Copyright 2018, the Royal Society of Chemistry. (c) withered leaves. Copied with permission [60]. Copyright 2017, the Royal Society of Chemistry. (d) spent tea leaves. Copied with permission [34]. Copyright 2023, Elsevier.

be hydrolyzed into glucose, aromatic aldehydes and organic acids, and then hydrothermally carbonized to form GQDs. The synthesized GQDs have an average size of about 3.9 nm with 2–3 graphite layers and exhibit highly selective quenching effect on Fe^{3+} ions. In addition, silica nanoparticles can be obtained *via* calcination of solid residues produced in the hydrothermal process, thereby increasing the economic benefits [59].

As a forestry waste, withered leaves of *Ficus racemosa* have a variety of plant components including organic acids, amino acids, lipids, and flavonoids. Different carbon nanomaterials (GQDs, amorphous carbon, and carbon nanofibers) can be formed due to various carbonization degrees during the hydrothermal reaction (Fig. 3c). Additionally, the multiple proteins and peptides in withered leaves contribute to the natural doping of carbon and nitrogen, which enhances the solubility and fluorescence of GQDs [60]. The simple one-pot hydrothermal method using source-rich feedstocks allows the large-scale preparation of high-quality crystalline GQDs.

Based on the hydrothermal method, the solvothermal technique uses chemical reagents instead of water as the solvent to synthesize GQDs. For example, Abbas *et al.* [34] used the green solvent "ethanol" instead of pure deionized water as the reaction solvent to prepare GQDs from spent tea leaves, obtaining a higher conversion yield (Fig. 3d). Ethanol acted as a graphitization and cleavage agent, generating hydroxyl radicals to facilitate C–C bond breaking during the heating. Similarly, lattice phosphorus-doped GQDs can be obtained from soy lecithin in ethanol through the solvothermal treatment. The successful lattice phosphorus doping is attributed to the *in-situ* reduction of lecithin by reducing agents generated by ethanol. The obtained GQDs have the high yield (71 wt%), high QY (0.54–0.73) and controllable emission wavelength (457–632 nm), which are appealing for fluorescence bioimaging [61].

2.2. Microwave-assisted synthesis

Microwave-assisted synthesis consists in rapidly converting the large amount of energy generated under microwave radiation into heat and thereby heating the precursor, which results in dehydration, polymerization, and finally carbonization to create carbon nanostructures [62]. Compared with other synthesis methods, microwave radiation can directly heat the target molecule, ensuring the higher-temperature reproducibility, more uniform heating, and obviously shorter reaction times. Microwave-assisted synthesis also supports the one-pot method for GQDs, leading to the high reaction efficiency and low associated costs. In addition, the microwave radiation provides the high yield and purity of GQDs.

Tran *et al.* [63] developed a microwave-assisted hydrothermal method, in which a passion fruit was heated at 170 °C for 20 min in microwave tubes to prepare N-GQDs with particle sizes of 3–12 nm. Nitrogen atoms present in passion fruit were successfully doped on the graphene structure of GQDs, strengthening the photovoltaic properties of N-GQDs. Tak *et al.* [64] synthesized GQDs with an average particle size of 10±1.3 nm by heating the extract of *Clitoria ternatea* flowers in a microwave oven at 900 W for 5–10 min. GQDs synthesized by this approach were stable and had potential for the treatment of Alzheimer's disease. Using the same method, GQDs can also be obtained from mango leaves by heating in a 900 W household microwave oven for 5 min. The resulting GQDs perceive high photostability and biocompatibility, exhibiting good cellular uptake [11]. Nevertheless, the size limitation of the microwave reactor hinders its application in large-scale reactions [65].

2.3. Pyrolysis and carbonization

Pyrolysis is one of the simplest carbonization processes, converting green precursors into GQDs at high temperatures. The pyrolysis conditions such as temperature, time and heating rate have significant effects on the structural and functional properties of the products [66]. In pyrolysis and carbonization, organic compounds are decomposed under oxygen-deficient high temperature conditions, leaving carbonaceous nanostructured GQDs.

In a typical carbonization process, the natural amino acid L-cysteine was heated to 215 °C for 30 min in an oil bath to prepare GQDs through a direct one-step carbonization. The sizes of

the obtained GQDs were in the range of 4–9 nm. There exist a variety of functional groups on the defective carbon ring and show a strong excitation-dependent emission [67]. Water-soluble N-GQDs were synthesized *via* pyrolysis using lemon juice at 200 °C for 20 min, whereby no harmful chemicals or solvents were consumed. Nitrogen atoms were successfully introduced into the graphitic framework of the prepared N-GQDs, which exhibited good stability, water solubility, and excitation-dependent down-conversion fluorescence [68]. Possessing no limits to purified organic small molecules, GQDs with sizes of 4.2–6.5 nm were produced by carbonization of a *Sarcopoterium spinosum* fruit extract, calcined at 350 °C for 2 h, exhibiting favorable antioxidant and antimicrobial properties [69].

Biomass can also be pyrolyzed at a higher temperature to produce carbon-rich solid products, from which GQDs are synthesized through a hydrothermal process whereby the structure of the carbonized products is aligned into a carbon core. For example, GQDs were produced *via* a two-step method using hemicellulose-rich peanut shell as the carbon source. In the first step, the peanut shell powder was stored at 200 °C to obtain a carbonaceous precursor. In the second step, the dispersion was transferred to a hydrothermal autoclave for 12 h at 280 °C to obtain GQDs. The GQDs had an average particle size of 6.1 nm and a QY of 14.3%, providing high selectivity and sensitivity for CEA detection based on label-free fluorescence [45].

2.4. Microplasma nanoengineering

Non-thermal and low-temperature plasma-based techniques, especially microplasma nanoengineering, are the simple, effective, and environmentally friendly approaches to synthesize GQDs without the need for toxic reagents and vacuum systems [70]. Compared with conventional plasma, microplasma is a compact, highly dense, and easy-to-integrate medium. High-concentration reactive radicals and other substances generated by plasma can cut the molecular structure of precursors, exhibiting great application potential in the synthesis of carbon-based nanomaterials and being very promising for the production of GQDs on an industrial scale [71,72].

Kurniawan *et al.* [73] used several bioresources as precursors (fructose, chitosan, CA, lignin, cellulose, and starch) to synthesize functionalized GQDs *via* microplasma method under the ambient conditions. Precursors with complex structures were prone to different degrees of fragmentation under the bombardment with reactive substances, leading to the generation of GQDs with different particle sizes and functional groups, as well as the wide distribution of band structures. In contrast, small molecules with uniform molecular weights grew homogeneously, generating GQDs with excitation-independent emission. In addition, it has been demonstrated that by extending the time of plasma treatment and increasing the applied discharge current, it is possible to increase the yield of GQDs and shift the emission toward the longer wavelengths corresponding to larger particle sizes [74,75]. Moreover, the pH level used in the synthesis of N-GQDs was shown to affect the concentration of $^{\bullet}OH$ radicals and e_{aq}^{-}. In particular, electrolytes with a lower pH produced fewer N-GQDs, whereas those with a greater pH exhibited the red-shift in the maximum photoluminescence intensity, providing valuable information for the green and controllable synthesis of GQDs [44].

2.5. Up-down joint synthesis

The synthesis of GQDs *via* high-temperature carbonization of biomass, combining the bottom-up approach to produce disordered carbon-based materials and the top-down approach to shear carbon-based precursors, ensures the large-scale production of inexpensive GQDs. The green top-down pathway is the key to the eco-friendly synthesis of GQDs.

The ultrasonically assisted method is based on the acoustic cavitation, in which the sound waves continuously generate microbubbles that collapse immediately, releasing a large amount of heat and pressure to precursor materials [32]. GQDs can be obtained by ultrasonically treating carbon sources. For example, GQDs were prepared *via* ultrasound-assisted mechanochemical cracking using Miscanthus as a carbon source. Graphene oxide (GO) and GQDs were synthesized *via* pyrolysis of Miscanthus at 1200 °C to form highly graphitic and aromatic biochar, followed by ultrasonic stripping in nitromethyl-2-pyrrolidone or water. In this case, GQDs were synthesized *via* ball milling and sonication treatment by cutting the biochar and GO into smaller units. Although the yield of such GQDs was low, it can be improved by selecting the appropriate operating conditions, making it possible to produce various graphene materials from biomass [42].

There are two main oxidation methods. One is the molecular oxidation which usually uses sulfuric acid, nitric acid, and other strong oxidants to produce GQDs with high yield and purity on the industrial scale [29]. However, the application and improper disposal of these oxidants may cause environmental pollution. Another pathway is the free radical oxidation (mainly including electrochemical oxidation and hydrogen peroxide) [76,77]. It is a clean, efficient, and relatively simple method, requiring a low content of reagents at a zero amount of by-products, which is in line with green synthesis strategies. Luo *et al.* [17] synthesized GQDs by heating the seaweed to 250 °C in a muffle furnace to obtain the carbonation products, which were then exposed to mild oxidation with H_2O_2. The GQDs, with a size distribution of 1–3 nm and a 1–5-layer graphene structure, were successfully used for the detection of 4-nitrophenol at low concentrations. In the electrochemical oxidation, there are generally two ways to generate GQDs: Using the precursor as an electrode and placing the precursor in a suspension. By controlling the applied potential, selective oxidation can be achieved in bulk materials [78]. The electrochemical oxidation is commonly used for oxidatively cutting the larger-scale graphitized carbon materials such as GO, CNTs, and coal. Although they can be used to synthesize GQDs from municipal solid wastes, such as batteries [79], they are rarely employed in the direct synthesis of GQDs from biomass. Consequently, the electrochemical oxidation is a reference green method in the generation of GQDs from green carbon materials such as biochar.

3. Properties of GQDs produced from biomass

3.1. Structural properties

GQDs are zero-dimensional nanomaterials typically composed of graphene nanosheets with lateral dimensions less than 10 nm and relatively low height, containing sp^2 and sp^3 carbon atoms. The GQDs can be triangular, square, hexagonal, or elliptical, but mostly possess oval or circular shape [80]. In addition, flower-like GQDs have also been reported [81]. Because of the small size, the electrical and optical characteristics of GQDs can be affected by various structural factors such as size and surface functional groups.

The properties of GQDs depend on their size, which is determined by the reaction time, temperature, and reactant concentration in the reaction process. Especially in the top-down approach, the GQDs usually exhibit a broad size distribution. By changing the conditions during synthesis, the shape and size of GQDs can be controlled. For example, when using rice flour as a carbon source in a green aqueous method, the increase in the heating time from 3 min to 10 min can control the growth of GQDs within a size range

of 2–6.5 nm, indicating that the extension of the polymerization time increases the size of GQDs [82]. Density functional theory (DFT) results reveal that size engineering can significantly alter the bandgap of GQDs, manifesting as a decrease in bandgap with the increase of transverse GQDs size [83].

The surface of GQDs is usually covered by the abundant oxygen-containing functional groups, such as carboxyl, hydroxyl, and epoxy groups. According to the synthetic route, a variety of defects, heteroatoms, and functional groups can be introduced to change the structure and characteristics of GQDs. To fine-tune the fluorescence properties of GQDs, as well as to change their electronic bandgap structure and improve their physicochemical properties, doping with metal and non-metal heteroatoms can be performed during the raw material preparation or post-processing [84]. For instance, nitrogen doping enhances the electronic properties, surface defects, and the fluorescence QY of GQDs due to the presence of surface groups. Sulfur doping results in longer emission wavelengths and red-shifting of GQDs, but reduces their fluorescence intensity. Boron doping creates a multitude of active sites that alter the optical properties of GQDs [85]. Besides, co-doping can also bring unique properties to GQDs [86]. In general, the purity of GQDs prepared from biomass is not high. Since some heteroatoms exist in biomass and its extract, the respective GQDs can be doped with some other elements, such as nitrogen, phosphorus and sulfur [12,38].

3.2. Optical properties

Different from other carbonaceous materials like graphene, the GQDs exhibit remarkable photoluminescence, dual photoluminescence and upconversion photoluminescence, which are on account of the quantum confinement. The spatial arrangement of hybrid orbitals endows GQDs with the outstanding fluorescent properties [24]. Besides, the GQDs primarily demonstrate the pronounced ultraviolet-visible spectra and photoluminescence excitation/emission characteristics.

3.2.1. Absorption property

The UV–vis spectrum of GQDs is due to the two types of transitions, namely $\pi \rightarrow \pi^*$ and $n \rightarrow \pi^*$, where the energy of $\pi \rightarrow \pi^*$ transition is higher than that of $n \rightarrow \pi^*$ transition [87]. Generally, GQDs exhibit strong light absorption around 230 nm in the ultraviolet region, which is because of the π-π^* transition of the C=C bond. For example, the UV–vis absorption spectrum of GQDs solution prepared using alkali lignin (AL) has an absorption peak at 257 nm, which can be found in AL, albeit at a shorter wavelength (229 nm). This means that GQDs have the high π-conjugated carbon integrity and can induce π-π^* transitions with the lower photon energy. A shoulder can be seen in the range of 270–390 nm upon the n-π^* transition between oxygen/nitrogen-containing groups and sp^2 aromatic domains [55]. While the tail of the absorption band is extended to the visible light spectrum, the broad emission band covers almost the entire visible range. On the whole, surface passivation, surface functional groups and edge defects have a synergistic effect on the emission and absorption peak positions of GQDs.

3.2.2. Fluorescence property

GQDs have tunable fluorescence properties resulting from their tunable band gap, surface defects, and jagged edges [77]. Moreover, GQDs have excellent optical properties such as fluorescence stability, up-conversion luminescence, and dual photoluminescence. Photoluminescence refers to the phenomenon whereby photons are absorbed by a substance and then re-emitted; thus, the non-zero band gap of GQDs plays a decisive role. The non-zero band gap of GQDs can be adjusted by changing their parameters such as size, surface functional groups, and surface morphology. When the size of GQDs prepared from CA *via* a green synthesis route is smaller than 4.22 nm, the photoluminescence is blue. As the size of GQDs is further increased, their photoluminescence turns to white. The photoluminescence intensity increases with the increase of GQDs size [88]. It has been established that the emission spectrum of GQDs undergoes a red shift with increasing size and passivation of surface functional groups. This red shift is caused by the changes in the positions of electrons and holes in GQDs. Furthermore, excitation wavelength, doping, defects, temperature, and solution pH also affect the luminescence behavior of GQDs [89].

The intensity of photoluminescence changes depending on the excitation wavelength, and the quantum confinement effect seems to be the most plausible reason for this phenomenon. To date, most biomass-derived GQDs exhibit the excitation-dependent luminescence emission, which may be caused by surface-emitting traps and defects. For example, GQDs prepared from starch through the green synthesis possess a typical excitation-dependent luminescence emission. With the increase in the excitation wavelength from 310 nm to 370 nm, the emission peak gradually shifts toward the longer wavelengths, while its intensity subsequently declines (Fig. 4a) [90]. This excitation-dependent feature may be due to different sizes of GQDs and/or different emissive sites of emission sites on GQDs [77]. Similarly, the fluorescence intensity of GQDs prepared *via* microwave from spent tea varied with the excitation wavelength [14]. In contrast, GQDs produced from CA with a uniform surface state exhibited the excitation wavelength-independent photoluminescence behavior (Fig. 4b) [91].

Moreover, the dopant atoms, the doping methods, and the structure all have an impact on GQDs. Wang *et al.* [13] used durian to prepare photostable S-GQDs and conducted the control experiments with undoped GQDs. According to the data, GQDs without dopant emitted within the much shorter wavelength range than S-GQDs, which can be attributed to the decrease in electronegativity caused by the S-lattice displacement charge injection effect. Zhang *et al.* [92] prepared GQDs from marigold granules and then added ethylenediamine to obtain N-GQDs. The results showed that under 365 nm UV light irradiation, the fluorescence color of N-GQDs turned from green to intense blue, proving that heteroatom doping can alter the fluorescence properties of GQDs (Fig. 4c). Adding different modifiers (tyrosine, L-arginine, urea, and K_3PO_4) in the one-pot hydrothermal process enriched the elemental composition of GQDs, enabling the synthesis of blue, green, yellow, and red luminescent GQDs (Fig. 4d) [50].

The temperature exerts a complex effect on the luminescence intensity. It has been demonstrated that an increase in temperature can induce a decrease in luminescence intensity, which is usually due to the nonradiatively trapped thermal activation caused by the interactions between excited electrons and phonons in the lattice [10,93]. However, according to the study on the synthesis of fluorescent GQDs from the honey, the increase in temperature weakened the non-covalent interactions between GQDs, forming the molecularly dissolved GQDs with enhanced fluorescence emission intensity [94].

GQDs generally emit a strong photoluminescence signal under the alkaline conditions, while their fluorescence intensity decreases in acidic media. With the increase of pH, the emission intensity of GQDs prepared from bamboo fibers increased monotonically, while their fluorescence properties in a strong acidic environment decreased respectively, which was due to the aggregation behavior of GQDs caused by the alkaline conditions [95]. The fluorescence intensity of N-GQDs prepared from melamine sponge and arjuna bark remained basically unchanged in the neutral pH range of 7–7.4. The fluorescence intensity decreased slightly even under highly acidic conditions, suggesting the application potential of N-GQDs in bioimaging (Fig. 4e) [43]. Particularly, GQDs prepared from plant extracts showed the pH-independent photoluminescence and

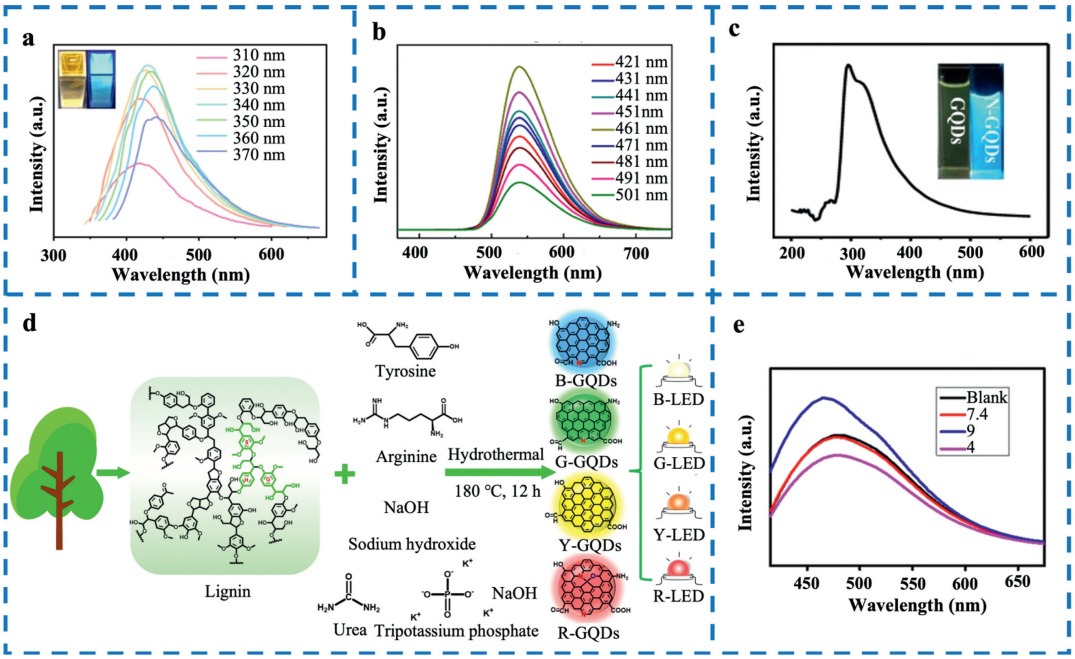

Fig. 4. Fluorescence properties of GQDs. Fluorescence spectra of GQDs at various excitation wavelengths with (a) excitation-dependent luminescence emission. Copied with permission [90]. Copyright 2022, Elsevier. (b) Excitation-independent luminescence emission. Copied with permission [91]. Copyright 2023, American Chemical Society. (c) UV–vis absorption spectrum of N-GQDs the inset highlights the fluorescence of GQDs and N-GQDs under a 365 nm ultraviolet lamp. Copied with permission [92]. Copyright 2019, Elsevier. (d) Multicolor GQDs synthesized from lignin. Copied with permission [50]. Copyright 2023, the Royal Society of Chemistry. (e) Emission spectra of N-GQD at pH of 4–9. Copied with permission [43]. Copyright 2022, Elsevier.

were highly stable in the pH range. This may be related to the highly stabilized structural morphology of GQDs, which remains unchanged in both alkaline and acidic media [9].

In addition, QY corresponds to the ratio of the number of photons emitted by the molecule at the excitation wavelength to the number of photons absorbed by the molecule. In general, the larger the QY is, the stronger the fluorescence or phosphorescence of the compound, which can indicate the effectiveness of the molecule as an imaging probe. To date, three factors have been proposed to enhance the QY, namely the inhibition of nonradiative recombination, the enhancement of photoluminescence centers through the edge modification, and the enrichment of structural electron density through the reduction [96]. Up till now, the QY of S-GQDs prepared from biomass was found to be 79%, exceeding that of most GQDs reported so far [12].

3.3. Cytotoxicity and biocompatibility

GQDs are used in biomedicine owing to their low cytotoxicity and impressive biocompatibility. Being the basic element of cells, carbon constitutes the skeleton of biomolecules. According to many studies, GQDs prepared from renewable feedstocks *via* green synthesis possess the better biocompatibility and stability along with lower toxicity compared to other nanomaterials [97]. The cytotoxicity of GQDs is thought to be caused through damaging DNA and upregulating certain proteins involved in cell cycle regulation. However, at concentrations below 100 μg/mL, GQDs typically possess zero toxicity [60]. Since specific application conditions limit the range of biocompatibility of GQDs, it is essential to evaluate the biocompatibility and biotoxicity of GQDs before their use for biological purposes. This can be done *via* implementing two types of experiments: *in vitro* and *in vivo*.

In vitro toxicity is often referred to as cytotoxicity, and most of current experiments aimed at testing biocompatibility are *in vitro* assays. There are two common methods for detecting cytotoxicity: methyl thiazolyl tetrazolium colorimetry assay (MTT) and lymphocyte proliferation assay (MTS). Both enable to assess cell viability and cell proliferation *via* colorimetry, whereas cytotoxicity is evaluated *via* cell survival and growth. GQDs have been shown to have negligible cytotoxicity against multiple cells, and differences in cytotoxicity are influenced by modifications of the surface [58,60]. MTT assays were performed on three cells with S-GQDs prepared from sugarcane molasses. The results showed that the toxicity of S-GQDs at 2 mg/mL for 24 h was mild, and all three cells exhibited the pronounced viability. The blood compatibility of S-GQDs was studied by *in vitro* hemolysis test. It was found that the red blood cell hemolysis rate of the material was 5%, and the agglutination was insignificant after 2 h, confirming that the material also had hemocompatibility [98]. The toxicity of N-GQDs from marigold granules to HeLa cells was evaluated *via* MTS. Once the concentration of N-GQDs rose to 1000 μg/mL, the cell viability reached 93%, significantly surpassing the concentration needed for cell imaging (200 μg/mL). Accordingly, the N-GQDs had the outstanding biocompatibility and low toxicity [14].

In vivo tests generally require the entire organism as the object of research. Tak *et al.* [99] employed male adult wistar rats weighing 220–250 g for the *in vivo* study of Alzheimer activity using Polygala tenuifolia-derived GQDs. The experimental method was legalized with the prior consent of the Institutional Animal Ethics Committee. Menezes *et al.* [100] examined the biological behavior of GQDs synthesized from CA *via* electrochemistry in healthy mice, which exhibited a widespread biodistribution, with the higher uptake of GQDs in the liver (>26%) and small intestine (>25%). Nevertheless, GQDs were not detected in major organs, and their low uptake in the brain confirmed the safety of the blood-brain barrier. Likewise, zebrafish was also used as the model animal for *in vivo* experiments [101]. Besides, it has been shown that GQDs in the cellular environment can generate the light-induced ROS due to the presence of oxygen-containing functional groups, as well as possess cytotoxicity, allowing for antimicrobial and anticancer applications [102,103]. In spite of numerous reports on the biological behavior of biomass-derived GQDs, most of them rely on *in vitro*

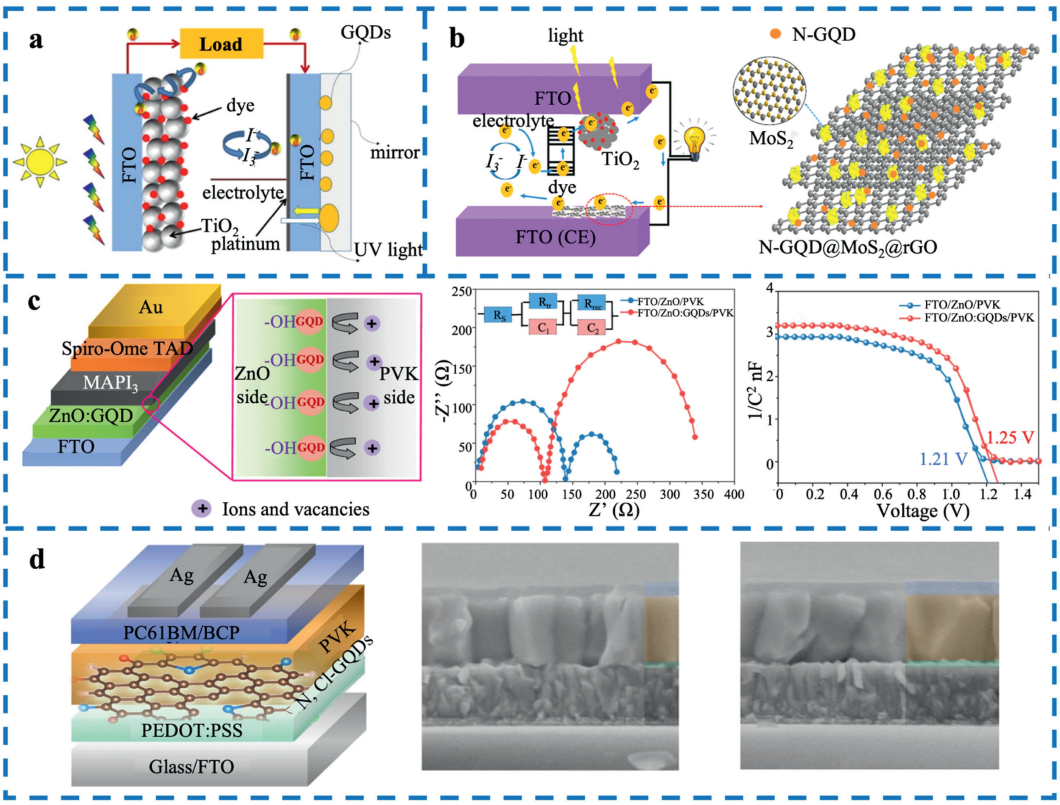

Fig. 5. Applications of biomass-derived GQDs in solar cells. (a) Possible mechanism of GQDs used as down-conversion material in DSSCs. Copied with permission [106]. Copyright 2018, Elsevier. (b) GQDs@MoS_2@rGO nanocomposite-based counter electrode for DSSCs. Copied with permission [108]. Copyright 2021, Elsevier. (c) ZnO/GQDs hybrid photoelectrodes used as ETLs in PSCs; Nyquist and Mott-Schottky plots of ZnO/GQDs. Copied with permission [109]. Copyright 2020, American Chemical Society. (d) Schematic structure of the PSC using N, Cl-GQDs; cross-sectional SEM image of the PSC: control and N,Cl-GQDs. Copied with permission [112]. Copyright 2022, Elsevier.

tests, whereas the data based on *in vivo* toxicity assessment are still scarce.

4. Application of biomass-derived GQDs

4.1. Energy conversion and storage

As the novel carbon-based nanomaterial, GQDs have the advantages of large specific surface area, multiple active sites, high electrical conductivity, tunable optical properties, and charge transfer. Consequently, they are promising for energy-related applications, such as supercapacitors, photovoltaics and light-emitting diodes. This section summarizes the recent advancement in GQDs prepared *via* green synthesis routes from biomass for energy conversion and storage.

4.1.1. Photovoltaics

Photovoltaics (PV) can convert safe, renewable solar energy into electricity without causing environmental pollution. Compared to graphene, GQDs have stronger interactions with surrounding molecules because of their edge atoms, rendering them suitable for PV applications, such as dye-sensitized solar cells (DSSCs), organic/inorganic hybrid solar cells, and perovskite solar cells (PSCs) [104]. However, in order to make PV a dominant component in the electricity market, the production costs should be further reduced [105].

Biomass-derived GQDs have excellent photoelectric properties at low cost and widely spread sources. For example, corn powder-derived GQDs exhibited significant brightness and successfully converted UV light into visible light with 450 nm and 520 nm wavelength. The GQDs can be applied to DSSCs as the down-conversion material (Fig. 5a). Compared with reference cells, solar cells modified with GQDs have the higher power conversion efficiency. Because of the down-conversion effect of GQDs, the cell was enhanced by 21% in J_{SC} [106]. However, the direct use of pure GQDs in DSSCs still faces many challenges. Chemically modified and functionalized GQDs endow DSSCs with high performance [107]. Silambarasan *et al.* [108] synthesized N-GQDs@MoS_2@rGO nanocomposites for DSSCs. The doping with nitrogen atoms increased the (n-type) charge transport in the GQDs and provided more active sites. After loading N-GQDs, the photoelectric conversion efficiency of the DSSCs device increased from 3.92% to 4.65% (Fig. 5b).

GQDs have been used as conductive carriers to improve the physicochemical properties of metal oxides. In order to address the instability of perovskite materials on the ZnO electron transport layer (ETL) during the annealing process, Ahmed *et al.* [109] prepared ZnO/GQDs composite photoelectrodes as ETLs in PSCs (Fig. 5c). GQDs acted as a protective layer passivating the oxidant on the ZnO surface and decreasing the recombination of electron-hole pairs, thus improving the stability of chalcogenide solar cells. The results showed that the PCE of the device was significantly increased from 10% to 17.65% after loading GQDs. This might have reduced the environmental impact of PSCs commercialization, making the latter economically feasible. Functionalized GQDs doped with elements and functional groups are also widely used in PSCs [110,111]. Guo *et al.* [112] rationally designed N/Cl doped GQDs for Sn-Pb-based low bandgap PSCs (Fig. 5d). N and Cl elements modulated the energy band structure and enhanced the p-type doping, which facilitated the interfacial charge distribution and passivated the defective states in Sn-Pb devices. The Sn-Pb-based PSCs exhibited an efficiency of 21.5%, retaining 90% of the initial

power conversion efficiency after 1000 h of operation. Functionalized GQDs provide an effective strategy for optimizing interfacial charge transport so as to enhance solar cell efficiency and stability.

4.1.2. Supercapacitors

Supercapacitors have aroused increasing interest as energy storage devices on account of their fast charging and discharging speed, long life cycle, and high energy density [113]. In theory, large specific surface area and low charge transfer resistance are critical to the capacitive performance of supercapacitors. Therefore, GQDs have great application prospects in high-performance supercapacitor materials owing to their excellent intrinsic properties [114].

A structure based on the all-lignin-converted GQDs and graphene sheet (GQDs/Gr) has been designed to produce supercapacitors with both fast charge-discharge capability and high specific capacitance. The constructed 0D/2D π-conjugated GQDs/Gr heterojunction system exhibited the impressive interfacial compatibility and conductivity, as well as numerous electronic capacitance sites and hierarchical channels. The results indicated that the GQD/Gr electrode had a capacitance of 404.6 F/g and a reaction time constant of 0.3 s, demonstrating a significant increase compared to those of the unmodified lignin electrode (160 F/g and 2.3 s, respectively) [115]. GQDs derived from marigold were electrodeposited on the working electrode to determine the specific capacitance and energy density. The test revealed that the electrode material had an elevated energy density (17.78 Wh/kg) and a power density (799.70 W/kg) with a specific capacitance of 200 F/g at 2.0 A/g, attributed to the abundant functional groups on the surface of the GQDs. Additionally, it still maintained the terrific capacitance retention after 1000 cycles [116].

Nowadays, flexible electronics, *e.g.*, wearable displays, have a wide range of applications. Hence, there is an ever-increasing demand for flexible and stretchable supercapacitors thanks to their ability to be well integrated with wearable systems, which has become a hot research direction for energy storage software [117]. Rice straw derived GQDs were used to prepare GQDs-enhanced stone waste particulates nanocomposites. The material exhibited the outstanding flexural strength (60 MPa) at low dielectric constant and high electrical conductivity [35]. The incorporation of GQDs introduced various interfaces enhancing electrical conductivity and flexural strength, thereby confirming the great potential of biomass for smart nanocomposite applications. Furthermore, GQDs have been used as active materials to enhance electrode supercapacitive performance. Citrate-derived N-GQDs and helical carbon tubes were employed to enhance the pseudocapacitive properties of MoS_2 for solid-state flexible supercapacitors. In this electrode structure, the multiple functional groups on the edge sites of N-GQDs played an essential role in improving the pseudocapacitance and wettability of the electrode materials. The findings showed that supercapacitors possessed a specific capacitance of 1893 mF/cm^2, excellent cycle life, favorable mechanical stability, and great flexibility [118].

4.1.3. Light-emitting diodes

What's more, the high electron mobility and strong luminescence characteristics of GQDs are also beneficial for the development of light-emitting diodes (LEDs) [119]. GQDs can be utilized in LEDs as novel phosphors, light converters, and down-conversion materials [90,120,121]. Among LEDs, white LEDs, which have the advantages of high efficiency, high brightness and energy-saving, have become one of the promising candidates for future solid-state lighting sources [122]. Plant leaves derived GQDs enriched with low-oxygen hydrocarbons exhibited high thermal stability, photostability, and pH stability without photobleaching, aggregation, and photooxidation. Using the GQDs as light converters, white light conversion caps were fabricated *via* red-green-blue color mixing for ultraviolet LEDs to generate white light [9]. Similarly, GQDs prepared *via* honey carbonization can also be employed in white light emission [94]. Intriguingly, the heteroatom doping can enhance the QY of GQDs and change their surface properties to provide the variable optical properties. Gao *et al.* [50] have successfully synthesized multicolor luminescent GQDs based on lignin by introducing different dopants. LED devices on the basis of GQDs can emit white, yellow, orange, and red light with LED conversion efficiencies of 13.3%, 11.3%, 7.1%, and 6.5%, respectively, and the irradiance of LEDs remains stable over a long period of time. This opens up new prospects for the synthesis of multicolor luminescent GQDs from biomass and their application to LEDs, contributing to the reduction of carbon footprint.

4.2. Environmental remediation

Pollutants, such as heavy metals, organic dyes and inorganic compounds, remaining in wastewater have strong color and durability which may affect the water ecosystem to a great extent. Therefore, the detection and elimination of pollutants from wastewater have become urgent tasks. Possessing a large specific surface area, abundant surface functional groups and high charge transfer properties, GQDs are considered an appealing option for this purpose.

4.2.1. Fluorescent nanoprobes

Contaminants in water have serious adverse effects on aquatic ecosystems. Nevertheless, high-cost and operationally complex detection methods are hardly able to meet the needs of real water quality testing [123]. Biomass-derived GQDs with photoluminescent properties, high water solubility, and biocompatibility offer a new platform for rapid and accurate monitoring of environmental pollutants. To date, GQDs have been used to fabricate fluorescent nanoprobes for the detection of a variety of ions, such as Hg^{2+}, Ag^{+}, I^{-}, and NO_2^{-}. These sensors have been chiefly developed by exploiting the affinity of certain functional groups of GQDs toward specific ions. For example, highly fluorescent GQDs prepared from biomass were applied in the three-channel sensitive detection of Fe^{3+} ions. It has been shown that GQDs have an obvious fluorescence decay, excellent linearity (0.995), and low detection limit (1.41 nmol/L) in the presence of trace Fe^{3+}. The high sensitivity of GQDs to Fe^{3+} is based on a synergistic dynamic quenching mechanism caused by the energy dissipation due to the amino-binding Fe^{3+} and the consumption of photogenerated electrons in competition [15]. Another study examined the luminescence intensity of prepared GQDs when exposed to 16 metal ions (10 mmol/L). The findings confirmed that among these ions, only Fe^{3+} and Cu^{2+} can quench the luminescence of GQDs, and the detected ion concentration displayed a fantastic linear relationship within the range of 0−1 μmol/L. The photoluminescence quenching mechanism may be related to the fast chelation kinetics and strong binding affinity of Fe^{3+} and Cu^{2+} to the N functional groups present in GQDs [124]. Pesticide residues in water can be detected by a similar quenching mechanism as metal ions. Hsieh *et al.* [125] developed B- and N-codoped GQDs as probes for paraquat detection in water. The remarkably high sensitivity of the photoluminescence quenching process is attributed to the formation of GQDs-(paraquat)$_x$ intermediates. Additionally, electrochemical and colorimetric sensors based on GQDs open new horizons for low detection lines and practical detection of contaminants [126].

4.2.2. Adsorption

GQDs can be taken as nano sorbents for the adsorption of pollutants. For example, GQDs prepared from waste bagasse were combined with folic acid and Fe^{3+}-tannic acid complex to form a

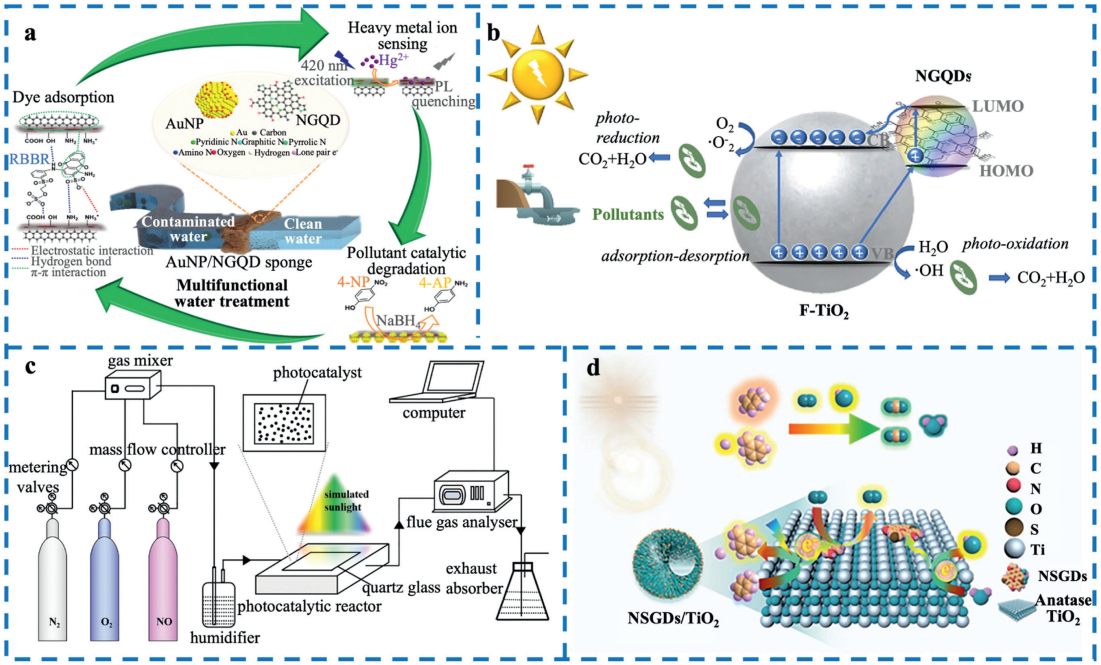

Fig. 6. Applications of biomass-derived GQDs in environmental remediation. (a) Excellent performance of NGQDs/AuNP composites in water treatment applications. Copied with permission [27]. Copyright 2023, Elsevier. (b) Proposed mechanism of F-TiO_2@N-GQDs photocatalytic degradation under UV–vis irradiation. Copied with permission [129]. Copyright 2023, Elsevier. (c) Photocatalytic system for NO degradation by GQDs/BWO. Copied with permission [130]. Copyright 2021, Elsevier. (d) Schematic of visible light-induced degradation of toluene by NSGDs/TiO_2. Copied with permission [131]. Copyright 2024, Elsevier.

supramolecular network. The large pore size of 38.35 nm endows the material with sufficient width to adsorb different pollutants. Therefore, this material can be utilized as an effective nanosorbent to remove heavy metal ions (Cr(VI)) and organic dyes (malachite green) from water at q_{max} values of 73.4 mg/g and 108.1 mg/g and removal rates of 99.5% and 94.8%, respectively, and validation experiments were conducted on real water samples. Such impressive results were mainly due to the hydrogen bonding, complexation, and electrostatic attraction between the adsorbents and the synergistic effect of the supramolecular network [127]. Similarly, Kurniawan *et al.* [27] synthesized pore-tunable N-GQD/AuNP nanocomposites with large surface area using chitosan as raw material, which exhibited excellent performance in water treatment. The concentration of adsorbed remazol brilliant blue R (RBBR) at 20 ppm was almost 100% within 120 min. In this case, the oxygen-containing and nitrogen-containing functional groups as part of N-GQDs generated the additional hydrogen bonds during the adsorption process, making N-GQDs able to induce π-π interactions with the benzene ring of RBBR, which enhanced the adsorption of the dye (Fig. 6a). Surprisingly, GQDs also have high efficiency in removing proteins, fluorides, drugs and even bacteria from water, thus making it possible to treat the industrial wastewater containing various pollutants [128].

4.2.3. Catalysis

Limited by regeneration and secondary treatment of adsorbents, catalytic technology is capable of degrading or transforming pollutants completely, leading to a new research boom in the treatment of environmental pollutants. The large specific surface area, quantum confinement effect and functional groups endow GQDs with unique optical and electronic properties, which have distinct advantages in photocatalysis and electrocatalysis. The hybrid system of N-GQDs combined with F-TiO_2 ensured effective photodegradation of diverse pollutants, including methylene blue (by 90%), ciprofloxacin (by 62%), and naproxen (by 60%). In this system, N-GQDs acted as electron reservoirs, which facilitated the efficient separation of electrons and holes, increasing the photocatalytic ability of F-TiO_2 (Fig. 6b) [129]. Not only restricted to pollutants in water, catalysis is considered a promising method for air purification as well. Cui *et al.* [130] combined the CA-derived GQDs with Bi_2WO_6 to initiate photocatalytic oxidation of air pollutant NO (Fig. 6c). Compared with a pure Bi_2WO_6, the conversion rate of the composite increased to 3.84 times, reaching 73% within 30 min, and the selectivity of NO_x^- formation achieved 88%. This is because of the favorable electron transfer ability of GQDs and the formation of a Z-type heterojunction in the composites, which enhanced the electron-hole separation efficiency of the catalysts. Volatile organic compounds (VOCs) can also be efficiently catalyzed *via* visible light induction. The NSGQDs/TiO_2 catalysts enabled 99.8% toluene degradation and 50% mineralization within 6 h, but also displayed universality to various VOCs (Fig. 6d) [131]. This S-scheme heterojunction efficiently separated photogenerated electron-hole pairs, in which nitrogen- and sulfur-codoped GQDs adjusted the bandgap to provide better light absorption and photoinduced charge carrier separation. Over and above, transition metal-modified GQDs exhibit the attractive possibilities in the catalytic conversion of the greenhouse gas CO_2 [132]. In particular, GQDs act to optimize the electronic structure, while transition metals are the real centers of CO_2 adsorption and activation.

5. Conclusion and perspective

GQDs have made tremendous progress in the fields of energy storage and environmental remediation due to their unique properties. However, most GQDs are prepared under energy-intensive synthetic conditions at high cost from fossil fuel-based precursors. Renewable biomass is a promising candidate for the production of GQDs, offering them a sustainable future. As a summary, this review highlights the preparation of biomass-derived GQDs by a green synthesis process. The inherent properties of GQDs can be utilized to enhance their performance in PV, supercapacitor, photocatalysis and other applications. A systematic review of green

synthesis methods, properties and applications of biomass-derived GQDs in recent years is presented.

Although some progress has been achieved in the green synthesis of GQDs from biomass in recent years, there is still a lot of room for improvement. In particular, to expand the application range of green synthesized GQDs, the following challenges must be overcome.

(1) Although green synthesis of GQDs consists in recycling waste resources, the collection and transportation of biomass require additional costs, and the yield of synthesized GQDs is still low. This requires the adequate technical routes and practical application to achieve a balance between the use and economic benefits.
(2) The synthesis of GQDs from biomass is often limited to the laboratory scale, and their production on an industrial scale has not yet been realized. To address this issue, it is crucial to find high-yield and economically viable biomass precursors as well as scalable and controllable green synthesis methods.
(3) Since the biomass contains impurities, the doping with different elements and multiple functional groups accompanying the GQDs pose a significant challenge to their mechanistic exploration. This requires a thorough investigation of elements present in precursors before preparation and characterization of GQDs.
(4) The properties of GQDs are affected by various factors, including size, dopants, edge configurations, and shapes. Moreover, the precise control of surface functional groups and morphologies of precursors is still a thorny problem due to the inherent properties and preparation methods of precursors. This necessitates the development of advanced synthetic methods for precise control according to specific application requirements. Alternatively, a fully automated approach combining machine learning and high-throughput synthesis may facilitate the discovery of GQDs with targeted properties.
(5) Functional modifications are crucial for the QY enhancement and bandgap tunability, some of which have been investigated but require further exploration. Furthermore, in terms of pollutant removal, the application of nanomaterials may cause secondary pollution, which should be comprehensively treated and separated in high purity.

Therefore, future research on green synthesis of GQDs from biomass should focus on addressing the above-mentioned challenges, developing advanced synthetic strategies, finding new raw materials with high optical properties and long emission wavelengths, improving the yield and QY of GQDs, and enhancing the performance and flexibility of the prepared devices. The application field of biomass-derived GQDs should also be expanded.

Declaration of competing interest

The authors declare that they have no known competing financial interests or personal relationships that could have appeared to influence the work reported in this paper.

CRediT authorship contribution statement

Tong Zhao: Writing – review & editing, Writing – original draft. **Ke Wang:** Data curation, Conceptualization. **Feiyu Liu:** Software, Methodology. **Shiyu Zhang:** Visualization, Resources. **Shih-Hsin Ho:** Supervision, Funding acquisition.

Acknowledgments

This work was financially supported by the following funding: National Natural Science Foundation of China (Nos. 52070057 and 51961165104), Project of a Thousand Youth Talents (No. AUGA2160100917), and Open Project of State Key Laboratory of Urban Water Resource and Environment, Harbin Institute of Technology (No. 2019DX09).

References

[1] X. Zou, M. Tang, Q.L. Lu, et al., Energ. Environ. Sci. 17 (2024) 386–424.
[2] Y. Li, Y. Shi, H. Wang, et al., Carbon Energy 5 (2023) e331.
[3] Z. Yang, T. Xu, H. Li, Chem. Rev. 123 (2023) 11047–11136.
[4] I.A. Kinloch, J. Suhr, J. Lou, et al., Science 362 (2018) 547–553.
[5] A.K. Geim, K.S. Novoselov, Nat. Mater. 6 (2007) 183–191.
[6] K.S. Novoselov, A.K. Geim, S.V. Morozov, et al., Science 306 (2004) 666–669.
[7] S. Caneva, M. Hermans, M. Lee, et al., Nano Lett. 20 (2020) 4924–4931.
[8] L.A. Ponomarenko, F. Schedin, M.I. Katsnelson, et al., Science 320 (2007) 356–358.
[9] P. Roy, A.P. Periasamy, C. Chuang, et al., New J. Chem. 38 (2014) 4946–4951.
[10] Z. Wang, J. Yu, X. Zhang, et al., ACS Appl. Mater. Interfaces 8 (2016) 1434–1439.
[11] M.K. Kumawat, M. Thakur, R.B. Gurung, R. Srivastava, ACS Sustain. Chem. Eng. 5 (2017) 1382–1391.
[12] G. Wang, Q. Guo, D. Chen, et al., ACS Appl. Mater. Interfaces 10 (2018) 5750–5759.
[13] R. Wang, G. Xia, W. Zhong, et al., Green Chem. 21 (2019) 3343–3352.
[14] A. Abbas, T.A. Tabish, S.J. Bull, T.M. Lim, A.N. Phan, Sci. Rep. 10 (2020) 21262.
[15] R. Wang, L. Jiao, X. Zhou, et al., J. Hazard. Mater. 412 (2021) 125096.
[16] Y. Wang, Q. He, X. Zhao, et al., J. Environ. Chem. Eng. 10 (2022) 107150.
[17] K. Luo, X. Luo, Y. Wu, et al., Diam. Relat. Mater. 135 (2023) 109849.
[18] L. Zheng, H. Zhang, M. Won, et al., Biosens. Bioelectron. 224 (2023) 115050.
[19] D. Ghosh, K. Sarkar, P. Devi, K.H. Kim, P. Kumar, Renew. Sust. Energ. Rev. 135 (2021) 110391.
[20] G. Li, Z. Liu, W. Gao, B. Tang, Coordin. Chem. Rev. 478 (2023) 214966.
[21] X. Ning, A. Hao, R. Chen, M.F. Khan, D. Jia, Carbon 218 (2024) 118772.
[22] Y. Yang, B. Wang, X. Zhang, et al., Adv. Mater. 35 (2023) 2211337.
[23] Z. Jin, M. Liu, X. Huang, et al., Anal. Chem. 94 (2022) 7609–7618.
[24] S. Tang, D. Chen, Y. Yang, et al., J. Colloid Interface Sci. 617 (2022) 182–192.
[25] S. Ye, F. Su, J. Li, et al., J. Mater. Chem. B 12 (2024) 122–130.
[26] Y. Ham, C. Kim, D. Shin, et al., Small 19 (2023) 2303432.
[27] D. Kurniawan, M.Ryan Rahardja, P.V. Fedotov, et al., Chem. Eng. J. 451 (2023) 139083.
[28] M.J. Im, J.I. Kim, S.K. Hyeong, B.J. Moon, S. Bae, Small 19 (2023) 2304497.
[29] A. Abbas, L.T. Mariana, A.N. Phan, Carbon 140 (2018) 77–99.
[30] L. Shi, B. Wang, S. Lu, Matter 6 (2023) 728–760.
[31] V. Dananjaya, S. Marimuthu, R. Yang, A.N. Grace, C. Abeykoon, Prog. Mater. Sci. 144 (2024) 101282.
[32] M.C. Biswas, M.T. Islam, P.K. Nandy, M.M. Hossain, ACS Mater. Lett. 3 (2021) 889–911.
[33] A.I. Osman, Y. Zhang, M. Farghali, et al., Environ. Chem. Lett. 22 (2024) 841–887.
[34] A. Abbas, S. Rubab, A. Rehman, et al., Mater. Today Chem. 30 (2023) 101555.
[35] A.K. Chaturvedi, A. Pappu, A.K. Srivastava, M.K. Gupta, Mater. Lett. 301 (2021) 130323.
[36] X. Chai, H. He, H. Fan, X. Kang, X. Song, Bioresour. Technol. 282 (2019) 142–147.
[37] W. Chen, J. Shen, G. Lv, et al., ChemistrySelect 4 (2019) 2898–2902.
[38] Z. Wang, D. Chen, B. Gu, et al., Spectrochim. Acta A 227 (2020) 117671.
[39] X. Zhong, C. Tong, T. Liu, et al., Biomater. Sci. 8 (2020) 6670–6682.
[40] L.V. Dutra, C.R. de Oliveira Fontoura, J.C. da Cruz, et al., Colloids Surf. A 651 (2022) 129442.
[41] H. Saleem, A. Saud, S.J. Zaidi, ACS Omega 8 (2023) 28098–28108.
[42] M. Safari, R.A. de Sousa, M. Salamat-Talab, et al., Appl. Sci. 11 (2021) 4846.
[43] R.V. Khose, P. Bangde, M.P. Bondarde, et al., Spectrochim. Acta A 266 (2022) 120453.
[44] D. Kurniawan, R.J. Weng, O. Setiawan, K.K. Ostrikov, W.H. Chiang, Carbon 185 (2021) 501–513.
[45] R.S. Tade, P.O. Patil, ACS Biomater. Sci. Eng. 8 (2021) 470–483.
[46] X. Li, G. Lin, L. Zhou, et al., Nanoscale Horiz. 9 (2024) 976–989.
[47] L.Y. Chang, C.C. Chang, M. Rinawati, et al., Appl. Energy 361 (2024) 122930.
[48] Y. Shen, Biomass Bioenergy 134 (2020) 105479.
[49] Y. Gong, L. Xie, C. Chen, et al., Prog. Mater. Sci. 132 (2023) 101048.
[50] T. Gao, S. Guo, J. Zhang, et al., Green Chem. 25 (2023) 8869–8884.
[51] T. Han, Y. Huang, T. Gao, et al., Food Chem. 404 (2023) 134509.
[52] T. Chen, J. Sun, N. Xue, et al., J. Mater. Chem. A 10 (2022) 10759–10767.
[53] Y. Zhu, L. Yan, M. Xu, et al., Colloids Surf. A 610 (2021) 125703.
[54] V.E. Bécsy-Jakab, A. Savoy, B.K. Saulnier, S.K. Singh, D.B. Hodge, Bioresour. Technol. 399 (2024) 130610.
[55] L. Zhu, D. Li, H. Lu, S. Zhang, H. Gao, Int. J. Biol. Macromol. 194 (2022) 254–263.
[56] R. Wang, W. Su, S. Zhang, et al., Adv. Opt. Mater. 11 (2023) 2202944.
[57] H. Guo, Z. Chen, Q. Yin, et al., Appl. Catal. B: Environ. 339 (2023) 123129.
[58] W. Chen, D. Li, L. Tian, et al., Green Chem. 20 (2018) 4438–4442.
[59] W. Wang, Z. Wang, J. Liu, et al., Ind. Eng. Chem. Res. 57 (2018) 9144–9150.
[60] M. Thakur, M.K. Kumawat, R. Srivastava, RSC Adv. 7 (2017) 5251–5261.
[61] G. Wang, A. Xu, P. He, et al., Mater. Lett. 242 (2019) 156–159.

[62] S. Głowniak, B. Szczęśniak, J. Choma, M. Jaroniec, Adv. Mater. 33 (2021) 2103477.
[63] H.L. Tran, V.D. Dang, N.K. Dega, et al., Sensor. Actuat. B: Chem. 368 (2022) 132233.
[64] K. Tak, R. Sharma, V. Dave, S. Jain, S. Sharma, ACS Chem. Neurosci. 11 (2020) 3741–3748.
[65] T.V. de Medeiros, J. Manioudakis, F. Noun, et al., J. Mater. Chem. C 7 (2019) 7175–7195.
[66] M. Wang, Y. Xie, Y. Gao, X. Huang, W. Chen, Bioresour. Technol. 395 (2024) 130364.
[67] C. Sudarsanakumar, S. Thomas, S. Mathew, et al., Mater. Res. Bull. 110 (2019) 32–38.
[68] M. Kaur, S.K. Mehta, S.K. Kansal, Sensor. Actuat. B: Chem. 245 (2017) 938–945.
[69] E. Turunc, O. Kahraman, A. Dogen, et al., Synthetic Met. 299 (2023) 117453.
[70] W.H. Chiang, D. Mariotti, R.M. Sankaran, J.G. Eden, K. Ostrikov, Adv. Mater. 32 (2020) 1905508.
[71] Z. Fan, H. Sun, L. Dou, et al., Chem. Eng. J. 461 (2023) 141860.
[72] D. Choi, H.J. Yeom, K.H. You, et al., Carbon 162 (2020) 423–430.
[73] D. Kurniawan, N. Sharma, M.R. Rahardja, et al., ACS Appl. Mater. Inter. 14 (2022) 52289–52300.
[74] J.S. Yang, D.Z. Pai, W.H. Chiang, Carbon 153 (2019) 315–319.
[75] D. Kurniawan, W.H. Chiang, Carbon 167 (2020) 675–684.
[76] H. Kalita, V.S. Palaparthy, M.S. Baghini, M. Aslam, Carbon 165 (2020) 9–17.
[77] D. Rai, Y. Jaiswal, S. Sinha, Appl. Surf. Sci. 653 (2024) 159386.
[78] S. Chung, R.A. Revia, M. Zhang, Adv. Mater. 33 (2021) 1904362.
[79] N. Kumar, M. Abubakar Sadique, R. Khan, Mater. Lett. 305 (2021) 130829.
[80] S.A. Ansari, Nanomaterials 12 (2022) 3814.
[81] A. Singh, R.K. Yadav, U. Yadav, T.W. Kim, Photochem. Photobiol. 98 (2021) 412–420.
[82] H. Kalita, J. Mohapatra, L. Pradhan, et al., RSC Adv. 6 (2016) 23518–23524.
[83] M. Fan, Z. Wang, K. Sun, et al., Adv. Mater. 35 (2023) 2209086.
[84] L. Zhu, D. Shen, C. Wu, et al., Ind. Eng. Chem. Res. 59 (2020) 22017–22039.
[85] B. Li, Y. Wang, L. Huang, et al., Synthetic Met. 276 (2021) 116758.
[86] M. Farahmand Habibi, M. Arvand, U. Schröder, S. Sohrabnezhad, Fuel 286 (2021) 119291.
[87] R.S. Tade, S.N. Nangare, A.G. Patil, et al., Nanotechnology 31 (2020) 292001.
[88] N. Far'ain Md Noor, M.A. Saiful Badri, M.M. Salleh, A.A. Umar, Opt. Mater. 83 (2018) 306–314.
[89] A. Alaghmandfard, O. Sedighi, N. Tabatabaei Rezaei, et al., Mat. Sci. Eng. C: Mater. 120 (2021) 111756.
[90] J. Yang, P. Li, Z. Song, et al., Appl. Surf. Sci. 593 (2022) 153367.
[91] Y. Zhao, B. Gu, G. Guo, et al., ACS Appl. Nano Mater. 6 (2023) 3245–3253.
[92] Y.P. Zhang, J.M. Ma, Y.S. Yang, et al., Spectrochim. Acta A 217 (2019) 60–67.
[93] H. Wang, R. Revia, Q. Mu, et al., Nanoscale Horiz. 5 (2020) 573–579.
[94] S. Mahesh, C.L. Lekshmi, K.D. Renuka, K. Joseph, Part. Part. Syst. Char. 33 (2016) 70–74.
[95] R.S. Tade, P.O. Patil, Curr. Appl. Phys. 20 (2020) 1226–1236.
[96] S. Zhu, Y. Song, J. Wang, et al., Nano Today 13 (2017) 10–14.
[97] H. Li, X. Yan, D. Kong, et al., Nanoscale Horiz. 5 (2020) 218–234.
[98] S. Sangam, A. Gupta, A. Shakeel, et al., Green Chem. 20 (2018) 4245–4259.
[99] K. Tak, P. Sharma, R. Sharma, et al., J. Drug Deliv. Sci. Tec. 73 (2022) 103486.
[100] F.D. de Menezes, S.R.R. Dos Reis, S.R. Pinto, et al., Mater. Sci. Eng. C: Mater. 102 (2019) 405–414.
[101] G. Gorle, G. Gollavelli, G. Nelli, Y.C. Ling, Pharmaceutics 15 (2023) 632.
[102] W. Wu, Y. Qin, Y. Fang, et al., J. Hazard. Mater. 441 (2023) 129954.
[103] X. Wang, C. Hu, Z. Gu, L. Dai, J. Nanobiotechnol. 19 (2021) 340.
[104] S. Sikiru, T.L. Oladosu, S.Y. Kolawole, et al., J. Energy Storage 60 (2023) 106556.
[105] A. Polman, M. Knight, E.C. Garnett, B. Ehrler, W.C. Sinke, Science 352 (2016) aad4424.
[106] H. Teymourinia, M. Salavati-Niasari, O. Amiri, M. Farangi, J. Mol. Liq. 251 (2018) 267–272.
[107] S. Mahalingam, A. Manap, A. Omar, et al., Renew. Sust. Energ. Rev. 144 (2021) 110999.
[108] K. Silambarasan, S. Harish, K. Hara, J. Archana, M. Navaneethan, Carbon 181 (2021) 107–117.
[109] D.S. Ahmed, M.K.A. Mohammed, S.M. Majeed, ACS Appl. Energ. Mater. 3 (2020) 10863–10871.
[110] E. Khorshidi, B. Rezaei, A. Kavousighahfarokhi, et al., ACS Appl. Mater. Interfaces 14 (2022) 54623–54634.
[111] Q. Cai, W. Sheng, J. Yang, et al., Adv. Funct. Mater. 33 (2023) 2304503.
[112] T. Guo, H. Wang, W. Han, et al., Nano Energy 98 (2022) 107298.
[113] J. Wang, X. Zhang, Z. Li, Y. Ma, L. Ma, J. Power Sources 451 (2020) 227794.
[114] N. Zahir, P. Magri, W. Luo, J.J. Gaumet, P. Pierrat, Energy Environ. Mater. 5 (2021) 201–214.
[115] Z. Ding, X. Mei, X. Wang, Nanoscale Adv. 3 (2021) 2529–2537.
[116] G.K. Gupta, P. Sagar, M. Srivastava, et al., Int. J. Hydrogen Energ. 46 (2021) 38416–38424.
[117] G. Shao, R. Yu, N. Chen, M. Ye, X.Y. Liu, Small Methods 5 (2021) 2000853.
[118] H. Wu, Z. Guo, M. Li, et al., Electrochim. Acta 370 (2021) 137758.
[119] S. Lee, J. Lee, S. Jeon, Sci. Adv. 9 (2023) eade2585.
[120] S. Jana, T. Dey, B.N. Shivakiran Bhaktha, S.K. Ray, Mater. Today Nano 24 (2023) 100400.
[121] H. Tetsuka, A. Nagoya, R. Asahi, J. Mater. Chem. C 3 (2015) 3536–3541.
[122] P. He, Y. Shi, T. Meng, et al., Nanoscale 12 (2020) 4826–4832.
[123] F. Liu, S. Zhu, D. Li, G. Chen, S.H. Ho, iScience 23 (2020) 101174.
[124] L. Wang, W. Li, B. Wu, et al., Chem. Eng. J. 300 (2016) 75–82.
[125] C.T. Hsieh, P.Y. Sung, Y.A. Gandomi, K.S. Khoo, J.K. Chang, Chemosphere 318 (2023) 137926.
[126] M.R. Mahajan, P.O. Patil, Inorg. Chem. Commun. 144 (2022) 109883.
[127] M.E. Mahmoud, N.A. Fekry, A.M. Abdelfattah, J. Mol. Liq. 341 (2021) 117312.
[128] M.E. Mahmoud, N.A. Fekry, S.M. Mohamed, J. Water Process. Eng. 46 (2022) 102562.
[129] I.J. Gómez, M. Díaz-Sánchez, N. Pizúrová, et al., J. Photoch. Photobio. A 443 (2023) 114875.
[130] Y. Cui, T. Wang, J. Liu, et al., Chem. Eng. J. 420 (2021) 129595.
[131] J. Tang, J. Zhu, L. Liu, et al., Chem. Eng. J. 482 (2024) 148813.
[132] K. Ghosh, N.K. Mridha, A.A. Khan, et al., Physica E: Low Dimens. Syst. Nanostruct. 135 (2022) 114993.